Iceland Liechtenstein Norway grants

Working together for a green, competitive and inclusive Europe

EMERALD

The Education, Scholarships, Apprenticeships and Youth Entrepreneurship

EUROPEAN NETWORK FOR 3D PRINTING OF BIOMIMETIC MECHATRONIC SYSTEMS

CASE STUDY #5

Project Title	**European network for 3D printing of biomimetic mechatronic systems 21-COP-0019**
Output	**IO4 - EMERALD e-case studies for project based learning method used in developing, testing and manufacturing of new biomimetic mechatronic systems by 3D printing technologies**
Module	**Case study #5 – Studies on 3D printed biomechatronic robotic gripper**
Date of Delivery	**September 2023**
Authors	**Filippo SANFILIPPO, Martin ØKTER, Filip GÓRSKI, Razvan PACURAR, Diana-Irinel BĂILĂ, Martin ZELENAY, Dan-Sorin COMSA, Paweł WOŹNIAK**
Version	**1.0, 30.09.2023**

Disclaimer: This result was realized with the EEA Financial Mechanism 2014-2021 financial support. Its content (text, photos, videos) does not reflect the official opinion of the Programme Operator, the National Contact Point and the Financial Mechanism Office. Responsibility for the information and views expressed therein lies entirely with the author(s).

Contents

1. Introduction

This document presents a description of a case study realized in the EMERALD project, as part of the IO4 work package. The case was selected on the basis of experience, possibilities, available solutions by the combined teams of University of Agder, Technical University of Cluj-Napoca, National University of Bucharest and Poznan University of Technology. Discussions conducted during various EMERALD project meetings were also taken into consideration and feedback of all partners was gathered and implemented.

The case study #5 focuses on a biomechatronic 3D printable robotic arm that can be used as a haptic device. The robotic arm was constructed as a project realized by University of Agder lecturers and students, as an educational example on how to construct and program simple robotic grippers. It has been used during the EMERALD project summer school in year 2022, in form of a toolkit available on GitHub platform [1], by students of all universities involved in the project consortium. Then, in the later phase of the project, the EMERALD consortium members realized material studies on the gripper, realizing 3D prints, tests and analyzes using various techniques and materials. This study is presented in this document.

Contents of this case study are also contents of a scientific paper, entitled “Use of high-performance polymeric materials in customized low-cost robotic grippers for biomechatronic applications: experimental and analytical research” by the same team of authors, submitted to journal Frontiers in Materials. At the moment of finishing the work in EMERALD project, the paper was not published yet, as such it is not cited in this study. It is noteworthy that the mentioned paper contains extensive material studies over PEKK material, which are not presented here (as the case study focuses on a specific device – robotic gripper). Reader is therefore encouraged to check on the paper to find more about material characterization.

2. Literature review and premises for the study

2.1. 3D printed robotic arms

Robotic arms have been an integral part of industrial automation, healthcare, and various other domains. The convergence of 3D printing technology with robotics has given rise to programmable robotic arms that offer enhanced versatility, cost-efficiency, and customization.

Various parts of robotic arms can be 3D printed, including joints, grippers, and even end-effectors. The ability to customize these parts to suit specific tasks is a notable advantage of 3D printing in robotics [2], with example of simple 3D printed parts shown in Figure 2.1.

Figure 2.1. Robotic arm parts 3D printed using low-cost FDM technology [2]

3D-printable robotics is characterized by its adaptability and customization. Robotic arms can be designed and printed to suit a range of applications, from educational platforms to industrial automation [3]. 3D-printed robotic arms have found a niche in education, enabling students and researchers to experiment with robotics and gain hands-on experience – which was also a point of this toolkit. The availability of DIY kits and open-source designs has democratized access to 3D-printable robotic arms, fostering innovation and experimentation in the robotics community [4].

3D-printed programmable robotic arms have made inroads into manufacturing, streamlining processes and increasing efficiency. They are used for tasks such as pick-and-place operations and quality control. In the medical field, these robotic arms can assist in

Disclaimer: This result was realized with the EEA Financial Mechanism 2014-2021 financial support. Its content (text, photos, videos) does not reflect the official opinion of the Programme Operator, the National Contact Point and the Financial Mechanism Office. Responsibility for the information and views expressed therein lies entirely with the author(s).

surgeries, offering precision and minimally invasive procedures. Rehabilitation and physical therapy applications are also emerging [3].

Current technology allows to use various 3D printing technologies in construction of low-cost robotic arms. As shown in previous chapters, many designs can be used as DIY projects, to create home-made or school-made robotics. Students and researchers interested in this topic may easily find many suitable projects, along with customization possibilities. Fused Filament Fabrication (FFF) is a versatile additive manufacturing method used to create 3D-printed robotic arm components, including grippers and whole arms. Several papers and research studies showcase the application of FFF for building functional robotic components.

A comprehensive review of robotic arm grippers is presented in the paper "Current Designs of Robotic Arm Grippers." This review discusses various designs of grippers, many of which can be created using Fused Filament Fabrication. It identifies benefits and drawbacks of different gripper designs, providing insights into the use of FFF for gripper fabrication [5].

In the paper titled "Design and 3D Printing of a Robotic Arm," the authors introduce the design concepts and the 3D printing procedure for a robotic arm created using 3D printing technology. While this paper primarily focuses on design concepts, it highlights the significance of 3D printing in the fabrication of robotic arms [6].

A paper titled "FDM Based Custom 3D Printer Development in Robotic" discusses the development of a custom 3D printer that can be utilized for robotic arm component fabrication. This research showcases the potential of 3D printers for creating robotic arm mechanical components with precision and low tolerances [7]. In "Current Designs of Robotic Arm Grippers," an underactuated adaptive 3D printed robotic gripper is presented. This gripper is designed for interactions with unpredictable environments and demonstrates the potential of 3D printing in creating adaptable robotic components, including grippers [8].

These papers and research studies underscore the use of Fused Filament Fabrication (FFF) as a viable method for creating robotic arm components such as grippers and whole arms. Researchers and robotics enthusiasts can explore these references to gain insights into the capabilities and applications of 3D printing in the realm of robotics.

Disclaimer: This result was realized with the EEA Financial Mechanism 2014-2021 financial support. Its content (text, photos, videos) does not reflect the official opinion of the Programme Operator, the National Contact Point and the Financial Mechanism Office. Responsibility for the information and views expressed therein lies entirely with the author(s).

2.2. Materials used in biomechatronic devices

A wide range of materials is nowadays available on the market, each offering particular advantages and disadvantages in the realization of biomechatronic devices [9,10]. High-performance FFF (Fused Filament Fabrication) materials, including but not limited to PEKK, has garnered significant attention for their outstanding mechanical properties [11-13]. These polymers possess exceptional strength, stiffness, and resistance to heat and chemicals, making them ideal candidates for applications demanding robustness and durability [14]. High-performance FFF materials outshine their standard Fused Filament Fabrication counterparts, such as PET-G, in terms of mechanical resistance, allowing for the creation of biomechatronic components which are capable of withstanding considerable stress and wear in these conditions [15,16]. However, the use of these materials is not without challenges. Precise temperature control is essential during the printing process, and issues like warping can pose difficulties, especially for intricate and large-scale designs [17,18]. Balancing the advantages with the complexities of handling these materials remains a key consideration in the case of biomechatronic applications [19]. The integration of carbon fiber composites into Fused Filament Fabrication (FFF) materials has expanded the scope of possibilities further on in several domains, including biomechatronics. Composites combine the versatility of FFF printing with enhanced mechanical properties, introducing newfound strength and stiffness [20-22]. Yet, this enhancement comes at a cost, both in terms of material expenses and the demands placed on the 3D printing equipment [23]. Finding the right balance between performance and affordability remains an ongoing pursuit for researchers and engineers in the field of biomechatronics [24]. On the other end of the spectrum, PolyJet technology represents one reliable alternative, employing UV resins to produce highly detailed, intricate structures with remarkable precision and smooth surface finishes [25,26]. This technology excels in creating visually appealing and intricately designed components, a quality particularly important in applications like customized prosthetics [27]. However, the mechanical characteristics of PolyJet materials may not always meet the rigorous demands of biomechatronic devices, where strength and durability are highly important [28]. Moreover, the initial and ongoing costs associated with PolyJet technology can be one disadvantage for those seeking cost-effective solutions [29,30].

Biomechatronic devices, including robotic arms place a unique set of demands on the materials used in their construction [31]. Mechanical characteristics such as flexural

Disclaimer: This result was realized with the EEA Financial Mechanism 2014-2021 financial support. Its content (text, photos, videos) does not reflect the official opinion of the Programme Operator, the National Contact Point and the Financial Mechanism Office. Responsibility for the information and views expressed therein lies entirely with the author(s).

strength, tensile properties, compressive and wear resistance are highly important in determining the performance and durability of these applications [32-34]. Robotic arms, for instance, rely heavily on bending and flexing to function effectively, directly influencing their lifting capacity and precision [35]. Consequently, the choice of materials for these devices must be made with thorough consideration of these mechanical characteristics [36]. To assess the justifiability of employing high-performance materials like PEKK in the development of customized robotic grippers for biomechatronic applications, the study was aimed to provide one comprehensive analytical and experimental approach. Analytical studies, including finite element analysis (FEA) have been utilized to simulate and optimize the mechanical behaviors of the components. Empirical research has been conducted to validate these analytical findings and to assess the performances of the robotic grippers that were taken into consideration in this research.

The study was aimed to provide an analytical and experimental research to provide one comparative analysis realized in the case of using high-performance materials like PEKK against conventional alternatives like PET-G and MED 857 (DraftWhite) materials, so one may comprise and understand both the advantages and challenges in utilizing these materials in the development of low-cost robotic grippers for biomechatronic applications by 3D printing technologies.

3. Materials and methods

3.1. Research concept and plan

The main concept of the presented case study was to answer the question if the use of the so-called high-performance 3D printing materials in production of customized robotic arms is justifiable by results of manufacturing processes and material tests. To answer that question, one high-performance material – PEKK – was selected and compared with two other popular materials (PET-G and MED 857 (DraftWhite) and technologies (FFF and Polyjet) by means of both analytical and empirical studies, based on previous knowledge and achievements of the authors.

In the initial phase of the research presented in this article, some materials and technologies were selected for the purpose of biomechatronic robotic devices. Then, by using a designed variant of an existing robotic gripper that was developed by part of the team of authors from the University of Agder (Norway) in previous studies [37-38] (Figure 3.1), parts of it were manufactured using various materials and have been subjected to strength tests emulating loading of a robotic arm. Simultaneously, the tests were performed using Finite Element Analysis, to check and compare analytical and empirical results. Various indicators were assumed to be used in order to compare selected materials and to answer the basic research questions. In this context has been considered the opportunity of considering, testing the mechanical behavior and using of new polymeric materials (like polyetherketoneketone - PEKK) for realizing of customized low-cost robotic grippers for biomechatronic applications. Regarding control algorithms for the proposed manipulator design, more details can be found in the following previously reported work and results [39-40].

The selected materials and technologies were: Fused Deposition Modelling, with PEKK (Polyetherketoneketone) as the test material and PET-G (Polyethylene Terephthalate Glycol) as control material, along with PolyJet technology, with DraftWhite (MED 857) UV resin material. Figure 3.2 shows the course of the research including the most important stages. Particular parts of the research are described in the next chapters of the article.

Disclaimer: This result was realized with the EEA Financial Mechanism 2014-2021 financial support. Its content (text, photos, videos) does not reflect the official opinion of the Programme Operator, the National Contact Point and the Financial Mechanism Office. Responsibility for the information and views expressed therein lies entirely with the author(s).

Figure 3.1. The robotic gripper 3D design [41]

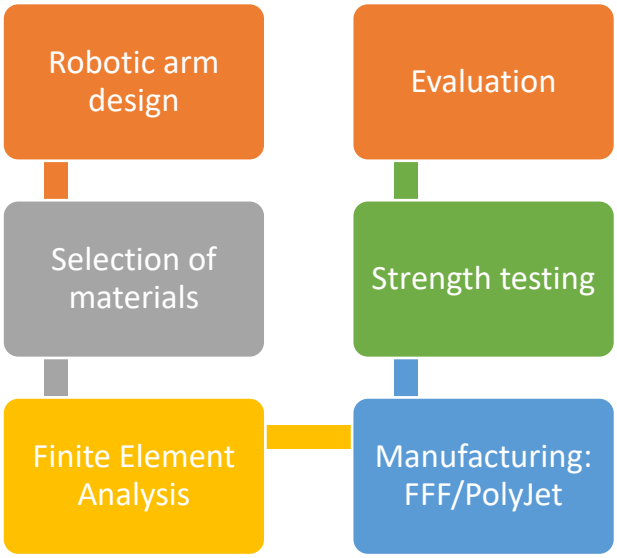

Figure 3.2. Course of the research described in the study

3.2. Robotic gripper project description

The primary goal of the project presented in this toolkit was to design an easy-to-build and assemble haptic installation that can function as a haptic device. This is achieved through the utilization of a joint with integrated springs. By employing this innovative approach, it becomes feasible to achieve greater motor displacement for a relatively smaller amount of force when compared to a rigid robotic arm. This design allows for enhanced tactile feedback and improved user experience in haptic interactions.

Contents of this chapter are mostly taken from the GitHub solution, available under [1].

The robotic gripper was designed in 3D CAD with typical assumptions for simple, one-axis robotic arms. The basic construction is presented in Figure 3.1 and the 3D models for 3D printing are available in the GitHub repository at [1]. Also, a full disassembly instruction, containing animations of all steps with names of standardized parts was prepared. It is available online, under link [42]. Examples of operations presented in the online instruction are presented in Figure 3.3.

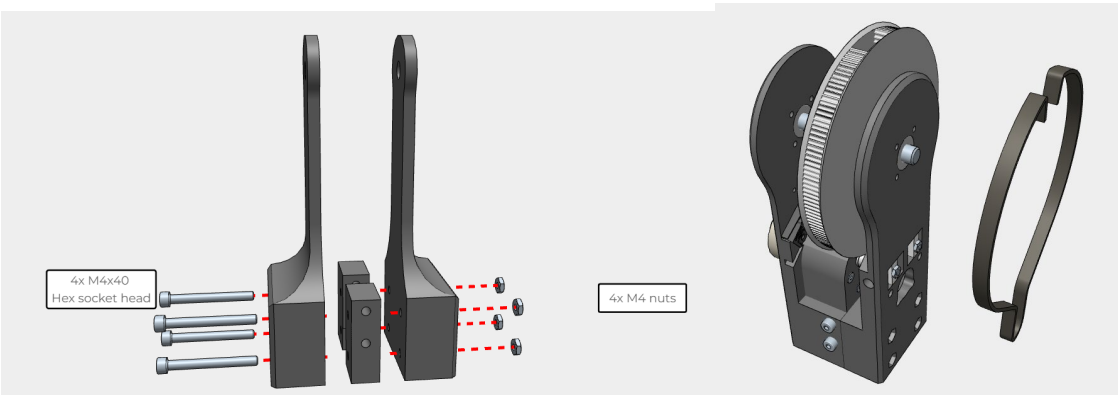

Figure 3.3. Disassembly instruction of the robotic arm, available at [42]

In robotic grippers used as haptic devices there are two main ways for control. Impedance control aim to steer the position by reading the motor force. Admittance control aim to control the force of the device by adjusting the position. This two are integrated as methods and can be used directly, By the use of the low level libaries these control codes may also be created by the user. A descriptive block diagram of the two control loops is presented in Figure 3.4.

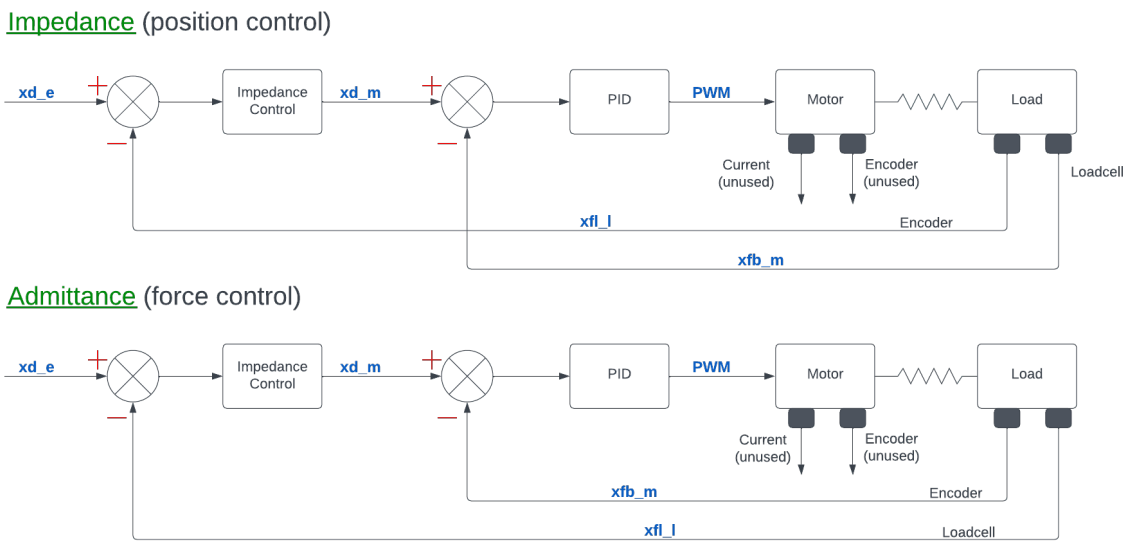

Figure 3.4. Control structure of the robotic haptic arm [1]

The software was built to be as modular as possible, aiming to ensure the easy operation of the robotic arm for users with varying programming backgrounds. The course is designed to cater to students with minimal to no prior experience in programming and control theory while also providing the opportunity for experienced personnel to conduct advanced control theory testing. For less experienced users, the steering library can be used, requiring adjustments only to control factor values. More experienced users have the option to build the control part themselves for implementing alternative steering methods. The basic libraries for data collection can be adapted and modified by experienced users to achieve optimal control, higher precision, and further system development.

The software comprises five classes. The AS5600 library, provided by Seed-Studio, facilitates the easy retrieval of data from the absolute magnetic encoder. Additionally, three low-level classes—PID, pwmMotor, and HapticSensor—are dedicated to data retrieval and the hard-coded control of the haptic arm. The final library, HapticArm, offers a variety of control methods based on control theory, utilizing the aforementioned classes for arm control. More details are available in [1].

The parts of the robot arm were 3D printed using the Fused Filament Fabrication technology, of PLA material. Using standard nuts and bolts, springs and other elements,

mechanical part and actuators were assembled. Using Arduino, sensors and other electronic components, the electronic part was assembled. The result is presented in Figure 3.5. Total of 4 arms were manufactured and successfully launched.

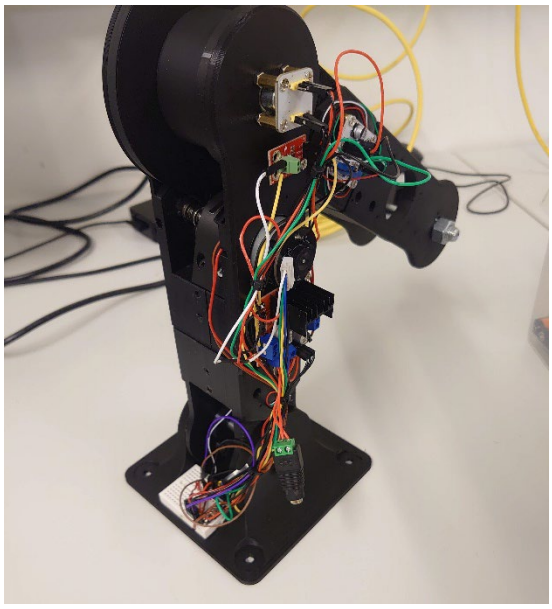

Figure 3.5. Assembled robotic arm made of 3D printed components [1]

Testing of the arm was also realized, checking correctness of movement and functioning as a haptic device. Some of its results can be found in a film, available under link [42] (Figure 3.6).

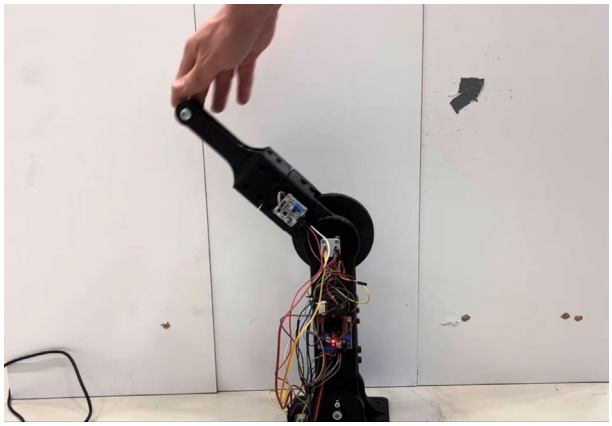

Figure 3.6. Haptic arm tests [42]

3.3. Finite element analysis to estimate the mechanical behavior of robot tooltip

The finite element analysis consists in the simulation of a bending test (Figure 3.7) with the aim of evaluating the strength characteristics of the robotic tooltip in three cases corresponding to different materials used for 3D printing: PET-G filament produced by Spectrum (PET-G Premium material characteristics datasheet. 2023), PEKK filament produced by Kimya (PEKK material characteristics datasheet. 2023), and MED857 (DraftWhite) material produced by Stratasys (MED 857 (DraftWhite) material characteristics datasheet. 2023). As shown in Figure 3, the tooltip components are assembled and placed in a clamping device. The bending effect is then produced by enforcing a vertical displacement of the threaded fastener placed at the free end of the tooltip.

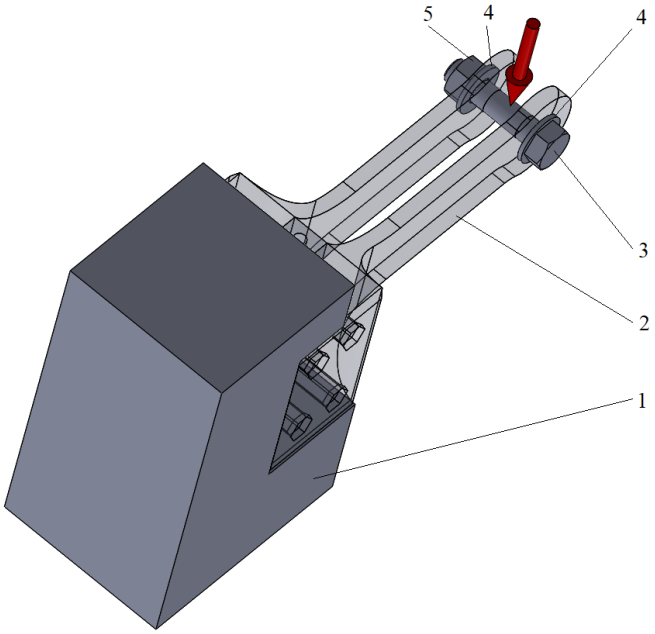

Figure 3.7. Principle of the bending test simulated for evaluating the strength characteristics of the robotic tooltip (1 – clamping device, 2 – robotic tooltip, 3 – screw, 4 – washers, 5 – nut, red arrow – vertical displacement of the threaded fastener)

The finite element model of the bending test was based on the following hypotheses:

- The components of the robotic tooltip are fully locked in the regions representing contact surfaces with the clamping device.

- The components of the threaded fastener (screw, washers, and nut – see Figure 1) are treated as rigid bodies.
- The components of the robotic tooltip are deformable bodies exhibiting an isotropic linear elastic behavior.
- The physical and mechanical properties of the analyzed materials (PET-G Premium material characteristics datasheet. 2023; PEKK material characteristics datasheet. 2023; MED 857 (DraftWhite) material characteristics datasheet. 2023) for the finite element model of the bending test were:
    - density (1270 [kg/m^3] for PET-G, 1261 [kg/m^3] for PEKK and 1175 [kg/m^3] for MED 857 (DraftWhite) material,
    - Elastic modulus (1950 [MPa] for PET-G, 2850 [MPa] for PEKK and 2200 [MPa] for MED 857 (DraftWhite) material,
    - Poisson's ratio (0.4 [-] for all considered materials,
    - Yield stress (48 [MPa] for PET-G, 80 [MPa] for PEKK and 45 [MPa] for MED 857 (DraftWhite) material.
- All the parts shown in Figure 3.7 were bonded together along their contact surfaces.

SolidWorks Simulation program was used for performing the Computer Aided Engineering (CAE) analyzes. For performing the CAE analyses to simulate the bending test for evaluating the strength characteristics of the robotic tooltip, several crucial details have been addressed to ensure accuracy and reliability of the results, such as:

- choosing of finite elements: For simulating the bending test, second-order tetrahedral elements have been utilized to ensure a high degree of precision in replicating the bending behavior of the robotic tooltip.
- meshing characteristics: the mesh was designed with smaller elements in areas of interest, such as the regions where bending stresses have been concentrated. For example, in the vicinity of potential stress concentrations, like the attachment points of the robotic tooltip, the element size was reduced to 0.5 mm, while in less critical areas it was increased to 1 mm. This approach ensured that the CAE realized analyses capture the finer details of stress distribution and deformation where needed while maintaining computational efficiency calculus being made.

The mesh consisted of 29798 second-order tetrahedral elements with a total number of 48949 nodes.

Disclaimer: This result was realized with the EEA Financial Mechanism 2014-2021 financial support. Its content (text, photos, videos) does not reflect the official opinion of the Programme Operator, the National Contact Point and the Financial Mechanism Office. Responsibility for the information and views expressed therein lies entirely with the author(s).

Applied forces: to closely mimic the real-world bending test, the CAE analysis applied forces that were consistent with the experimental results. In the actual experiment, maximal forces recorded were approximately 500 N for PET-G, 1000 N for PEKK, and 1600 N for MED857 (DraftWhite) material. Similarly, in the CAE analyses, these forces were replicated to maintain fidelity with the experimental conditions. This alignment of forces ensured that the CAE results were directly comparable to the physical tests, allowing for a meaningful assessment of the robotic tooltip's strength characteristics.

3.4. Additive manufacturing methods used for producing and testing of robotic tooltip

To empirically test the difference in using PEKK material for robotic end effector construction as opposed to standard materials such as PET-G and MED 857 (DraftWhite) materials, the end effector was manufactured additively using varying processes and materials. For each manufactured set of parts, 3 aspects were assessed: manufacturing process (stability, assembly fit), economical aspect (manufacturing time and total cost) and strength (maximum force recorded at the bending test). There was no manufacturing parameters variability between samples made of the same material. The products were manufactured using the Fused Filament Fabrication (FFF) technology, with two different materials – PET-G and PEKK, as well as Jetted Photopolymer (PolyJet) technology, using one, standard material MED 857 (DraftWhite) which is an UV resin. Three sets of robotic tooltip pieces were manufactured of each material (a single set consisting of 2 tooltip parts and 2 spacers).

The manufacturing was realized using the following machines and parameter setting:

- FFF technology, PET-G material samples – FLSun Super Racer machine (Zhengzhou Chaokuo Electronic Technology Co., China) with delta type kinematics, with a working chamber sized Ø260 x 330 mm. For printing the samples made of PET-G material, the extrusion temperature of 250°C, table temperature: 70°C, extrusion velocity: 40 mm/s layer thickness: 0,25 mm, infill density: 30%, 4 outlines, 4 bottom/top closing lines were used as main parameters.
- FFF technology, PEKK material samples – Intamsys Funmat Pro 410 (INTAMSYS Technology Co. Ltd, Shanghai, China) with regular kinematics and build chamber sized 305 x 305 x 406 mm. For printing the samples made of PEKK material, the

extrusion temperature: of 380°C, table temperature: 130°C, chamber temperature: 90°C, extrusion velocity: 25 mm/s, layer thickness: 0,25 mm, infill density: 30%, 4 outlines, 4 bottom/top closing lines were used as main parameters.

- PolyJet technology – Stratasys MediJet J5 machine (Stratasys Ltd., Minnesota, USA), with circular working chamber (max part size up to 140 x 200 x 190mm) and 18 micron layer thickness.

The PEKK material filament had to be additionally dried prior to manufacturing. The drying process was realized using laboratory drier oven SLW 53 made by POL-EKO company in Poland. The drying, as recommended by the material producer, was realized in 100°C for 10 hours and then for an additional 3 hours in 150°C. Manufacturing commenced directly after drying, with no cooling period.

For comparison of the different materials and processes, economic coefficients were also determined after printing. Using a standard method of calculating cost of additively manufactured products applied in previous researches by the authors, e.g. in (Górski et al. 2020, Górski et al. 2021), the costs of printouts of different technologies and materials were compared. The following formula was used for cost calculation:

$$c_p = c_{mac} * t_m + c_{mat} * m_p + c_w \qquad (1)$$

where:

c_p – total cost of produced part, USD,

c_{mac} – cost of machine usage (taking into account amortization cost - purchase cost per 2 years of continued usage - and electrical energy consumption), USD/h,

t_m – time of manufacturing (layer deposition only) [h],

c_{mat} – cost of material, USD/g

m_p – mass of used material [g],

c_w – additional work cost, USD (estimated – taking into account pre- and post-processing operations – drying, cleaning etc.)

It is noteworthy that the calculation was realized in a non-commercial manner – only the basic, objectively determined costs were accounted for, not including margin (profit) of potential manufacturer.

3.5. Mechanical testing setup experiments

The strength testing of the manufactured samples consisted of a destructive quasi cantilever beam bending test of the assembled robotic end effector tooltip, manufactured additively of PET-G, PEKK and MED 857 (DraftWhite) materials. The strength tests were performed with the universal strength testing machine Sunpoc WDW-5D-HS (Sunpoc, Guiyang, China). The tooltip was assembled using standard metric nuts and bolts and constrained together at the testing machine rail using additional metal supports. Tooltip ends were also connected with a nut and bolt. The whole tooltip assembly was considered as a single sample in the testing experiments. The machine loading effector was placed in the middle, to simulate loading of the tip. The whole set, immediately before testing, is presented in Figure 3.8.

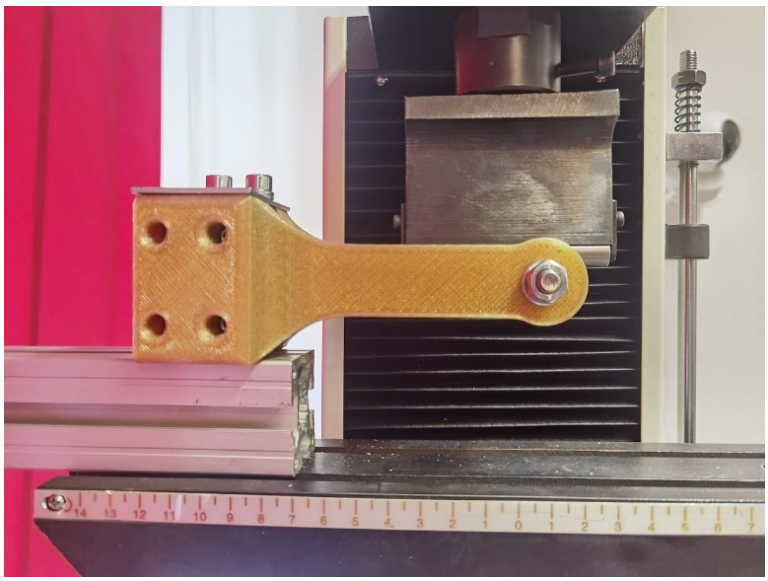

Figure 3.8. Strength testing setup of a PEKK printed sample using universal testing machine

The result of each test is a course of a load–displacement diagram, obtained from the used strength testing machine. The test was carried out until the sample was destroyed (by cracking) or visibly deformed. Speed of movement of the loading end was 10 mm/min.

To be able to compare obtained results with the FEM analyses, the stress in the main (narrow) part of the tooltip was determined analytically, by using a formula for stress

calculation in beams subjected to bending. The experiment was a typical scenario of a cantilever beam – constrained at one end, with force applied at the other, free end. For the sake of the analysis, the geometry was simplified – it was assumed that there is a beam of 70 mm length, with two rectangular cross-sections of 25x5 mm, separated with a 12,7mm space, constrained at one end and loaded at the other end. These assumptions are presented in Figure 3.9.

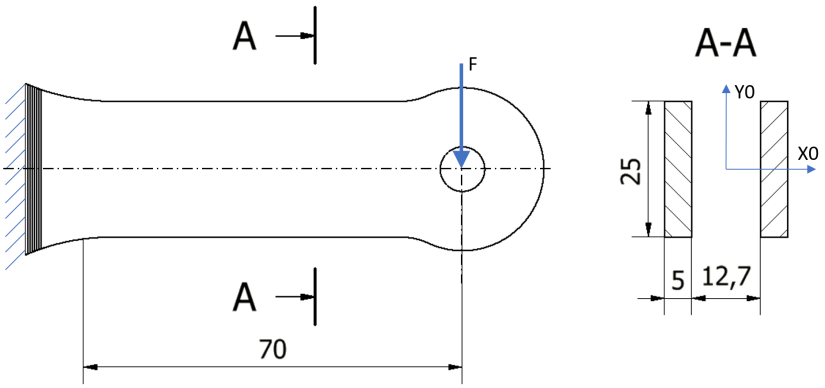

Figure 3.9 Loaded part treated as a cantilever beam – basic assumptions and dimensions

Using a standard, analytical method of determining static stress in the loaded beam, well known in available literature, e.g. [43] (Gere and Goodno, 2012), the following formula was used for stress calculations:

$$\sigma_b = \frac{M_b y}{I_{cx}}$$

where:

σ_b – bending stress under specific load [MPa]

M_b – bending moment, calculated as $P * l$, where P – loading force [N] and l = 70 [mm],

y – the distance from the beam's neutral axis to the point of interest along the height of the cross section [mm]

I_{cx} – centroidal moment of inertia of the beam's cross section, calculated as a sum of two rectangular cross-sections, using dimensions of the tooltip main part (section A-A in Figure 3.9) [mm^4].

4. Results

4.1. Finite Element Analysis results

The finite element model allowed the determining of the critical values in case of the vertical displacement which has been applied at the free end of the robotic tooltip at which the maximum value of the von Mises equivalent stress becomes equal to the yield stress of each material, respectively at 14 mm in case of PET-G material, 18.8 mm in case of PEKK material and 26.2 mm in case of MED 857 (DraftWhite) material. Figure 4.1 lists the maximum values of the von Mises equivalent stress $\sigma_{eq,max}$ determined by the SolidWorks Simulation finite element program in case of values of the vertical displacement d enforced at the free end of the robotic tooltip that were mentioned.

As one may notice in Figure 4.1, the maximum von Mises equivalent stress that was reached at the level of the tooltip components was 48.1 MPa in case of PET-G material (Figure 10 (A), 84,7 MPa in case of PEKK material (Figure 4.1 (B) and 47.7 MPa in case of MED 857 (DraftWhite) material (Figure 4.1 (C)).

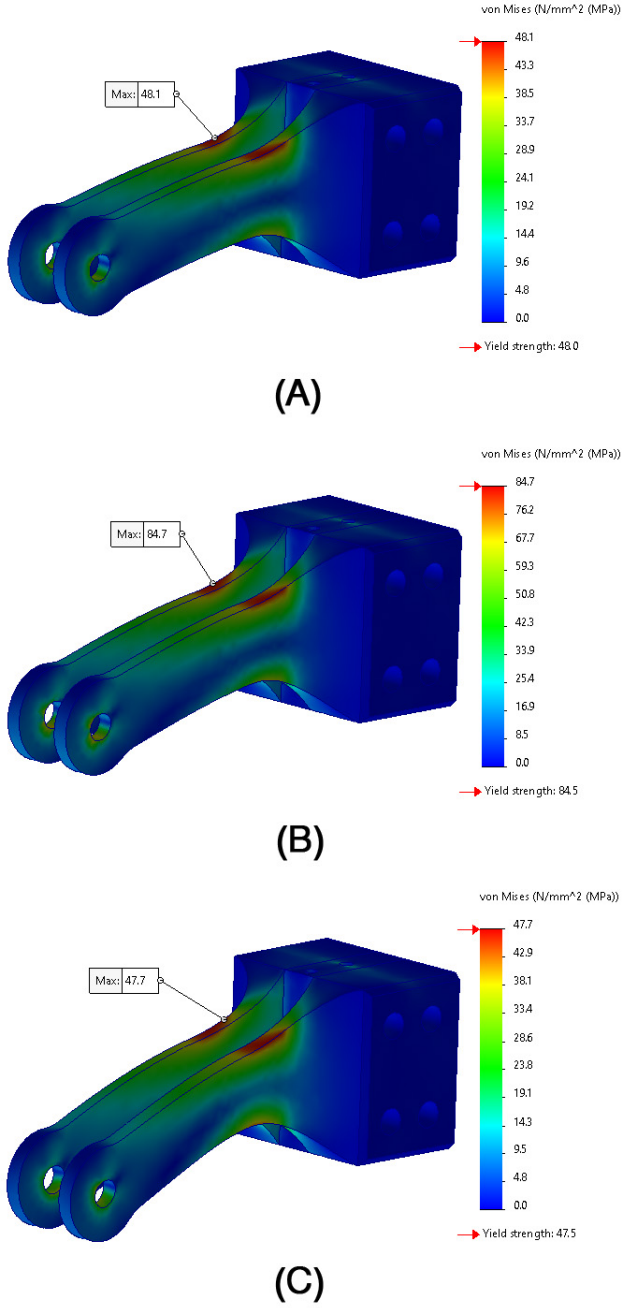

Figure 4.1. Distribution of the von Mises equivalent stress at the level of the tooltip components (A) made of PET-G, as obtained by enforcing a vertical displacement of 14 mm; (B) made of PEKK, as obtained by enforcing a vertical displacement of 18.8 mm and (C) made of MED 857 (DraftWhite), as obtained by enforcing a vertical displacement of 26.2 mm.

Disclaimer: This result was realized with the EEA Financial Mechanism 2014-2021 financial support. Its content (text, photos, videos) does not reflect the official opinion of the Programme Operator, the National Contact Point and the Financial Mechanism Office. Responsibility for the information and views expressed therein lies entirely with the author(s).

4.2. Manufacturing results and process economic coefficients

Of the performed manufacturing processes, 100% succeeded, without any major errors, concerning all the aspects (machine, software, code and material). The images presented in Figure 4.2 show sets of parts manufactured using various materials and technologies. The parts were visually examined to find any major or minor errors of representation of their shape and surface.

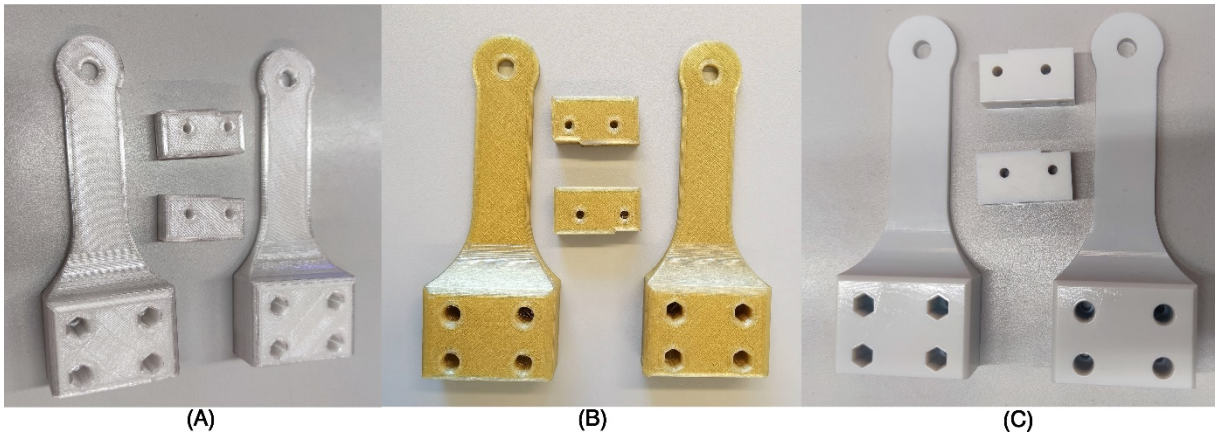

(A) (B) (C)

Figure 4.2. Manufactured samples, (A) FFF, PET-G material; (B) FFF, PEKK material; (C) PolyJet, MED 857 (DraftWhite) material

Regarding the manufacturing processes and their comparison, the following observations can be made:

- The FFF manufacturing process using PET-G material shown in Figure 4.2, (A) went smoothly without any noticeable errors or problems. The manufactured parts are free of visual and shape errors, with noticeable, expected staircase effect and surface roughness. Also, due to applied infill of 30%, they are considerably lightweight – it does not affect the long part of the tooltip, only the bulk, lower part.
- The FFF manufacturing using PEKK material shown in Figure 4.2, (B) was also done without any disturbances and the parts do not present any major errors or inconsistencies. However, it is noteworthy that the process took much more time – layer deposition was very long, as well as material preparation (drying in a dedicated furnace).

Disclaimer: This result was realized with the EEA Financial Mechanism 2014-2021 financial support. Its content (text, photos, videos) does not reflect the official opinion of the Programme Operator, the National Contact Point and the Financial Mechanism Office. Responsibility for the information and views expressed therein lies entirely with the author(s).

- The PolyJet process of samples shown in Figure 4.2 (C) also went smoothly without any disturbances. The obtained parts were very smooth and precisely represent the part geometry, without visible staircase effect, having a partially shiny surface thanks to low layer thickness. They were also considerably heavy and rigid – the standard PolyJet process settings do not allow openwork internal structure, so the parts are monolithic. For all the materials, fitting and assembling the complete tooltip was not a problem. Acceptable accuracy was obtained, although the least visual looseness was noted for parts made of PolyJet technology, which was to be expected due to high machine accuracy and very low layer thickness.

The summary of economic coefficients of the printouts is presented in Table 1.

Table 1. Time and cost of manufacturing for the three considered materials

Material / process Parameters	PET-G (FFF)	PEKK (FFF)	MED 857 (PolyJet)
Layer deposition time	7 hr 9 min	17 hr	5 hr 7 min
Total manufacturing time (est.)	7 hr 30 min	31 hr*	6 hr
Build material consumption [g]	104	105	293
Build material cost (USD)	$ 1.81	$ 60.52	$ 67.82
Machine operation cost (USD)	$ 1.75	$ 44.28 *	$ 468.37
Total manufacturing cost (USD)**	**$ 8.19**	**$ 109.44**	**$ 547.77**

* including the drying process

** including cost of work of human operator – pre- and post-processing

The following observations can be made related to the time and cost indicators of the considered processes in comparison:

- FFF manufacturing out of PEKK material is the longest process of all three tested, both in terms of layer manufacturing (more than 2 times longer than using PET-G material, but also 3 times longer than the MED 857 (DraftWhite) material and preprocessing (13 hours of drying). As the material is also costly and requires a special, expensive machine to process, this variant is significantly, 13 times more expensive than standard FFF 3D printing of PET-G material.

- In terms of the PolyJet process – it is in total much shorter than manufacturing of PEKK and even standard FFF process (PET-G material). It is also noteworthy that in the PolyJet technology, horizontal increase in build chamber filling with more parts does not considerably increase build time – for a single set of samples it was approx. 5 hours, for two sets – 6,5 hours, for three – approx. 8 hours). Considering a very low layer thickness (18µm) and high infill (monolithic, non-controllable), efficiency of PolyJet process can be considered as very high.
- The PolyJet machine has an immense purchase cost, by a large margin, which makes the process the most expensive of all with the assumed calculation methodology (5 times more expensive than PEKK and almost 70 times more expensive than standard FFF 3D printing of PET-G material).
- It can be observed that for the MED 857 (DraftWhite) material and the PolyJet process, consumption was much higher than in the case of FFF processes. Of the 293 g consumed by the PolyJet device, however, only 226 g are actually used for building the part, the rest is wasted (machine uses all 6 installed cartridges and purges them during each print). It is still a considerably larger amount than in the case of FFF processes – however, in PolyJet there is no partial internal filling, meaning that the parts are monolithic. This does not influence the beam part of the tooltip, as it has low wall thickness – however the bulk part of the tooltip is affected and the parts of PolyJet are considerably heavier due to that fact.
- All three processes and materials allow achieving acceptable results in terms of process stability, as well as lack of major errors in shape and accuracy, enabling proper fit. As the cost difference between typical, easily accessible FFF process and the two other (high-performance) processes is significant, it seems not advisable to use these for regular production of customized robotic arm parts, unless dedicated properties of high-performance materials (such as chemical or thermal resistance, as well as increased strength) are to be utilized.

4.3. Mechanical test experiments results

In the case of all the samples, the bending test was realized without disturbances. Most samples were broken entirely during the tests, with an exception of all PET-G material samples, which cracked, but did not disjoint. The experiment was always stopped shortly after decrease of loading force was observed, hence lack of full failure of samples of these materials. Also, one sample of MED 857 (DraftWhite) material was not visibly cracking – heavy plastic deformation occurred, but without breaking the continuity of material. All the other samples of the batch failed at comparable loads and the failure was similar in observation to the "brittle fracture" mechanism, with sharp edges and smooth surfaces at the locations of failure.

Figure 4.3 (A), (B) and (C) presents juxtaposition of samples made of PET-G, PEKK and MED 857 (DraftWhite) material after the test.

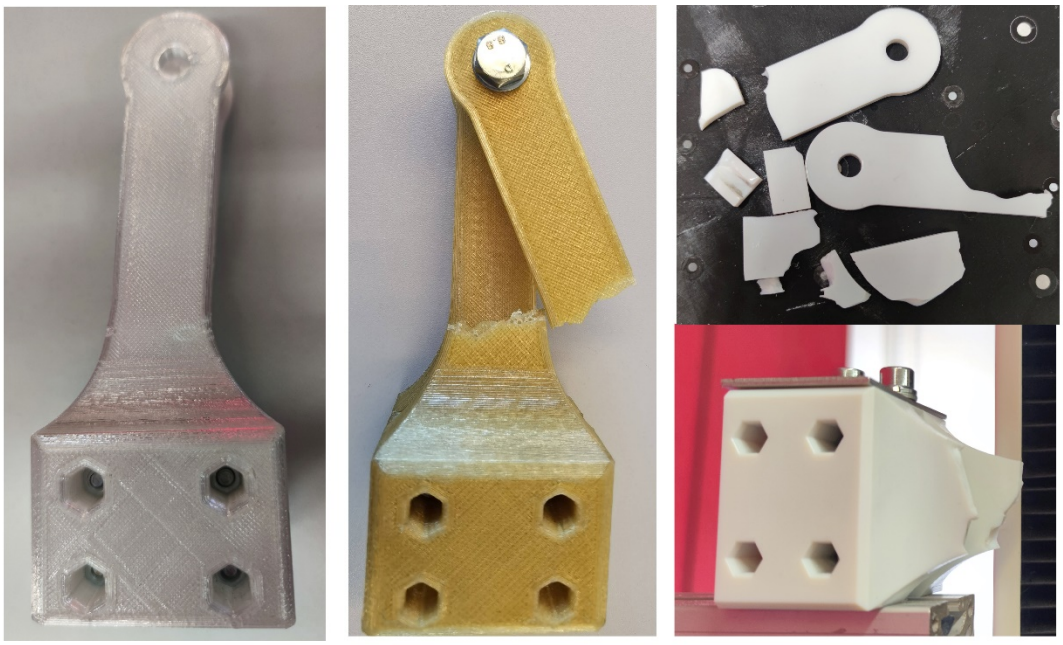

(A) (B) (C)

Figure 4.3. Samples made of (A) PET-G, (B) PEKK and (C) MED 857 (DraftWhite) materials after strength testing

Figures 4.4 (A), (B) and (C) present examples of load-displacement diagrams for all three materials, obtained from the testing machine software.

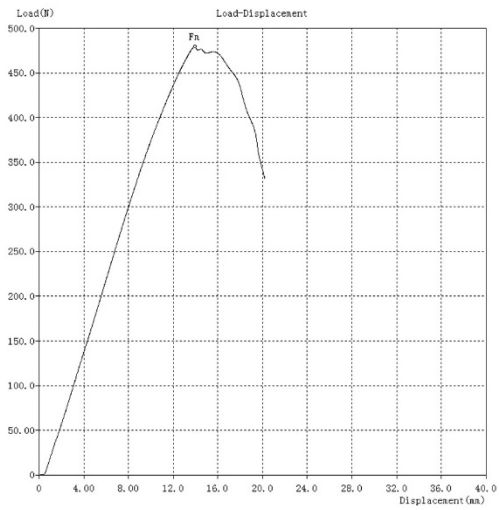

(A)

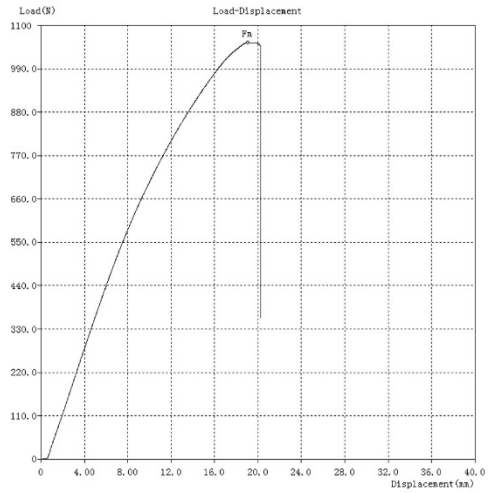

(B)

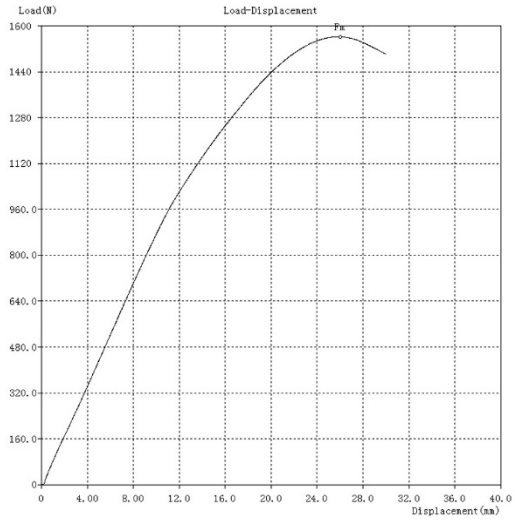

(C)

Figure 4.4. Load-displacement diagram for samples made of (A) PET-G, (B) PEKK and (C) MED 857 (DraftWhite) materials

Table 2 presents the main numerical results of strength testing, calculated on average for 3 samples – maximal registered forces, forces at break, maximal displacements and maximal stresses calculated using the formula shown in earlier chapters.

Table 2. Results of strength tests of robotic arm grippers made of different materials

Materials and characteristics	F_{max} [N]	F_{break} [N]	d_{max} [mm]	σ_b [MPa]
PET-G	472.5	298.5	21.25	31.8
PEKK	1047.0	986.5	21.05	70.4
MED 857	1547.7	1494.5	29.20	104.0

Analyzing the results, the following observations can be made:

- As one may notice by examining Figure 4.2, the abscissae corresponding to the maxima of the load-displacement curves resulting from experiments are well approximated by the previously mentioned numerical (CAE) results that were presented in Figure 10 .
- As expected, performance of PEKK samples is considerably higher than PET-G samples – more than twice a load was achieved before failure of the part.
- Displacements at maximum load are almost the same for both filament materials – and almost 40% higher for the MED 857 (DraftWhite) material. This type of material which is based on resin also was less prone to fracturing.
- The PEKK material samples, as opposed to PET-G samples, broke almost instantaneously and the failure was visible at the whole cross-section (of a single beam). It might be considered more of a brittle fracture than plastic deformation in this case. In the case of PET-G, much more plastic behavior was observed, with no visible breaking of the beam parts, but with heavy plastic deformation instead.
- The Med 857 (DraftWhite) material was the strongest, by a large margin (more than 50% difference when comparing with the PEKK material). Also, the highest displacement was achieved in this case. This may be partially attributed to monolithic infill of the part, making it heavier in total – but also thanks to the low layer thickness and different method of layer deposition,

the connections between layers may be stronger than in FFF technology, resulting in higher performance under load.

Comparison of mechanical characteristics in terms of strength obtained in the experiment and declared by the producer brings interesting observations. For the PET-G, experimental value (31 MPa) was twice lower than the declared value of 64 MPa. For the PEKK material, declared and experimental values were comparable (experiment – slightly less than declared, at 70 MPa versus approx. 80 MPa as declared). However, for the MED 857 (DraftWhite) material, the obtained strength (100 MPa) was considerably higher than the declared value (70-85 MPa). The discrepancy in this case might be a result of simplifications during stress calculations, but only to a certain extent – this does not fully justify almost 30% of difference between material sheet data and experimental data. More experiments on different geometries would be needed to be performed in the future regarding the mechanical characteristics and behavior of this material.

4.4. Discussion

In the experimental studies, it was found that the PEKK material – which is a high-performance material used for additive manufacturing by material extrusion – indeed has much better strength properties than generic materials used in regular 3D printing processes, like PET-G and MED 857 (DraftWhite) materials. The difference is considerable – the material is able to sustain at least twice the load, with the same deformation, as compared to the standard PET-G material. At the same time, the PEKK material processing using material extrusion 3D printing is not troublesome, provided appropriate temperature conditions are used – which is still not common in the case of other high-performance materials (e.g. like in the case of composite filaments with carbon fibers). The manufacturing of this material is a stable and repeatable process, requiring almost no post processing. The obtained parts present acceptable visual quality and shape accuracy, enabling proper assembly of obtained machine parts.

However, costs of production in the case of this material – as well as with other materials of this group are very high. The PEKK material, as of current market availability, is 30 times more expensive than regular FFF filaments (such as PET-G or MED 857 materials). Also, it requires considerably more expensive and less available machines to perform the

processing. Totally, cost of producing the robotic gripper parts as presented in this article was 13 times higher for PEKK than of a standard material. Another disadvantage is drying time, which is almost as long as manufacturing (in the case of parts considered in this article) and also much longer than the whole production process using the filaments not needing the drying.

As such, the authors believe it is only advisable (in practical conditions), if typical FFF filaments do not allow to obtain proper loading strength – however, in such case it could be advisable to change part geometry, instead of highly increasing production cost by using a very expensive material. Another scenario of use would be if typical materials do not fulfill special criteria, e.g. of temperature or chemical resistance. Only then would it be practical to use PEKK as a replacement.

The comparison of the FFF technology with the PolyJet technology also brought some interesting insights. The PolyJet machine is a very expensive device and its purchase and operation costs vastly increase the total cost of obtained parts. However, if the machine costs were taken aside, the material itself (which is a generic UV resin supplied by the machine producer) is actually less expensive than PEKK. At the same time, it excels at each criterion taken into account in this article – the parts are very strong (more than 50% stronger than PEKK parts and more than 3 times stronger than PET-G parts, in the conducted experiment), accuracy and surface quality are much better than in FFF (almost no staircase effect visible, with a shiny, smooth surface without additional processing) and the production time is also shortest of all three processes considered in the article. It might be considered practical more than PEKK (or other high-performance polymers) if the PolyJet machine is readily available (thus, taking the purchase cost out of the equation) – in a shorter time, parts of better characteristics can be obtained.

The PolyJet process also has certain disadvantages. Aside from the enormous price, the material waste is quite high – extra material is consumed of all cartridges, regardless of batch size (the material waste is even larger when considering that FFF filaments are fully recyclable, while polymerized UV resin – not as much). Considering also that times of manufacturing do not increase significantly while adding more parts to the batch (provided that maximal vertical dimension, i.e. layer amount, stays the same), it would be advisable in practical conditions to produce as large batches as feasible when dealing with that technology. Also, internal filling cannot be reduced (or otherwise controlled), as such the

Disclaimer: This result was realized with the EEA Financial Mechanism 2014-2021 financial support. Its content (text, photos, videos) does not reflect the official opinion of the Programme Operator, the National Contact Point and the Financial Mechanism Office. Responsibility for the information and views expressed therein lies entirely with the author(s).

parts can be bulky – proper geometry would need to be obtained, taking these considerations into account. In terms of the strength – the parts were very durable during the experiment described in this article, however from the author's experience – this may not be the case with small geometry parts and lower wall thicknesses. Further examinations on various parts and materials would need to be done to further decide if PolyJet can excel over FFF and in which applications, in terms of strength.

Anyhow, the experiment has proven that it is certainly possible to manufacture customized robotic arms using 3D printing technologies. The robotic gripper presented in the article is just an exemplary device – of course in the case of mass production, additive technologies would not be feasible. But in the case of highly customized devices, such as robotic prosthetic hands, legs or exoskeletons and their parts, additive manufacturing may be the way to go. Therefore, it is important to know if the currently available high performance materials and processes allow obtaining parts of considerable strength and accuracy. The experimental and analytical results state that this is the case.

Disclaimer: This result was realized with the EEA Financial Mechanism 2014-2021 financial support. Its content (text, photos, videos) does not reflect the official opinion of the Programme Operator, the National Contact Point and the Financial Mechanism Office. Responsibility for the information and views expressed therein lies entirely with the author(s).

5. Summary

In this article, it was presented how the high-performance materials and 3D printing technologies like Fused Filament Fabrication (FFF) or Polyjet technology can be used to produce an exemplary biomechatronic device – part of a robotic gripper.

In terms of CAE analysis, the results obtained from finite element simulations, showed that each of the analyzed materials (PET-G, PEKK and MED 857 (DraftWhite) exhibited a consistent, incremental rise in stress, reflecting their escalating response to enhanced loading. This information has been considered crucial as it signifies the distinct mechanical resilience and capabilities of PET-G, PEKK-A, and MED 857 (DraftWhite) materials, thereby aiding in the informed selection of materials for specific load-bearing applications in robotic tooltips. The observed trends underscore the heightened stress tolerance of PEKK-A and MED 857 (DraftWhite) materials as compared to PET-G, influencing their preference in high-performance applications.

Based on results that were reached through mechanical testing experiments which were in close correlation with the ones reached through CAE analyses that were realized, it was possible to determine that PEKK, despite its superior performance compared to PET-G, exhibited brittle fracture characteristics, snapping suddenly under load, contrary to the more plastic deformation that has been observed in case of other tested materials like PET-G. The resilience of MED 857 (DraftWhite) markedly overshadowed others, supporting loads over 50% higher than PEKK and showcasing the least susceptibility to fracturing, attributing to its monolithic infill and stronger inter-layer connections from a distinct layer deposition method. An interesting divergence between experimental and declared mechanical strengths was noted, particularly in the case of PET-G and MED 857 (DraftWhite) materials. While PEKK's experimental and declared values aligned closely, PET-G's experimental strength was half the declared value, and MED 857 (DraftWhite) exceeded its declared strength by almost 30%, signaling possible simplifications in stress calculations or the need for further diversified geometrical testing to ascertain the material's mechanical characteristics comprehensively. In terms of 3D printing processes, crucial insights into the practicalities and challenges of each method have been provided. FFF manufacturing with PET-G and PEKK materials went seamlessly; producing parts with acceptable accuracy and no major errors, with a noted staircase effect and surface roughness in case of PET-G material. PEKK, while offering quality outputs was notably time-intensive and costly, making it a less

Disclaimer: This result was realized with the EEA Financial Mechanism 2014-2021 financial support. Its content (text, photos, videos) does not reflect the official opinion of the Programme Operator, the National Contact Point and the Financial Mechanism Office. Responsibility for the information and views expressed therein lies entirely with the author(s).

feasible choice for regular production. The process demands prolonged layer deposition and material preparation time, leading to significant production delays in the manufacturing process. In contrast, the PolyJet process offers enhanced efficiency, yielding smooth and highly accurate parts, demonstrating its superiority in achieving detailed geometrical representation and fine layer thickness. This precision, however, comes at a steep cost. Despite its shorter manufacturing time, the high purchase and operational costs of the PolyJet machine make it the most expensive among the tested processes, presenting a barrier for its adoption in regular production of robotic parts. Furthermore, the PolyJet process results in substantial material consumption and wasting materials during the print. This, coupled with the creation of monolithic, heavier parts, underscores the limitations of this technology, despite its evident advantages in precision and finish.

In a cost and time-effective analysis, while all processes deliver satisfactory results in terms of stability and accuracy, the financial and time investment required for PEKK and PolyJet processes does not align with their output benefits for regular production of robotic arm parts. The utilization of these high-performance processes would only be judicious if specific, advanced material properties are imperative for the application, emphasizing the need for a balanced consideration of cost, time, and material performance in selecting the suitable manufacturing process. In the further studies, it would be worth performing other tests on high-performance materials, such as fatigue tests, tests of chemical and temperature resistance, dimensional accuracy studies and others. Also, a second direction of studies should include producing actual biomechatronic devices (such as orthoses or prostheses) and testing their use with real patients, to provide more answers about practical possibilities of using the current generation of 3D printing technologies in current trend with the new types of materials that are expanding and occurring on the market. The results related to this case study in particular has been published as a joint article of the EMERALD consortium in Frontiers in Materials journal (any section or information undertaken from this case study report has to be accompanied by a citation / reference to the next following article: Păcurar R.I., Sanfilippo F., Økter M.B., Băilă D-I, Zaharia C., Nicoară A.I., Radu I.C., Savu T., Górski F., Kuczko W., Wichniarek R., Comşa D.S., Zelenay M. and Woźniak P. (2024), Use of high-performance polymeric materials in customized low-cost robotic grippers for biomechatronic applications: experimental and analytical research. Front. Mater. 11:1304339. doi: 10.3389/fmats.2024.1304339).

Disclaimer: This result was realized with the EEA Financial Mechanism 2014-2021 financial support. Its content (text, photos, videos) does not reflect the official opinion of the Programme Operator, the National Contact Point and the Financial Mechanism Office. Responsibility for the information and views expressed therein lies entirely with the author(s).

Literature

1. https://github.com/Microttus/HapticSommerSchool/tree/main, access: January 2023
2. https://www.instructables.com/3D-Printed-Robot-Arm/
3. Marín Garcés, J.; Veiga Almagro, C.; Lunghi, G.; Di Castro, M.; Buonocore, L.R.; Marín Prades, R.; Masi, A. MiniCERNBot Educational Platform: Antimatter Factory Mock-up Missions for Problem-Solving STEM Learning. Sensors 2021, 21, 1398. https://doi.org/10.3390/s21041398
4. https://all3dp.com/2/3d-printed-robot-arm-diy-robotic/
5. Hernandez, Jaime & Sunny, Md. Samiul & Sanjuan, Javier & Rulik, Ivan & Islam, Ishrak & Ahamed, Sheikh & Ahmed, Helal & Rahman, Mohammad. (2023). Current Designs of Robotic Arm Grippers: A Comprehensive Systematic Review. Robotics. 12. 5. 10.3390/robotics12010005.
6. Kitsakis, Konstantinos & Petrou, Nick & Tanos, Ilias & Kechagias, John. (2016). Design and 3d Printing of a Robotic Arm.
7. Prianto, E., Herliansyah, M. K., Pramono, H. S., Husna, A. F., Adam, R., & Raditya, A. E. (2022, December). FDM Based Custom 3D Printer Development in Robotic Arm Mechanical Prototype Printing. In *Journal of Physics: Conference Series* (Vol. 2406, No. 1, p. 012005). IOP Publishing.
8. Hernandez, J.; Sunny, M.S.H.; Sanjuan, J.; Rulik, I.; Zarif, M.I.I.; Ahamed, S.I.; Ahmed, H.U.; Rahman, M.H. Current Designs of Robotic Arm Grippers: A Comprehensive Systematic Review. Robotics 2023, 12, 5. https://doi.org/10.3390/robotics12010005
9. Segil, J. (2018). Handbook of Biomechatronics. 1st Edition, Elsevier, ISBN: 9780128125397
10. Barrera, S., A., Blanco, O., A., Martínez, R., E., Gómez, B., F.A., Abúndez, P., A., Campos, A., R.; Guzmán,V., C. H. (2022). State of the Art Review of Active and Passive Knee Orthoses, Machines 2022, https://doi.org/10.3390/machines10100865
11. Wasti, S., Adhikari, S. (2020). Use of Biomaterials for 3D Printing by Fused Deposition Modeling Technique: A Review., Front. Chem.,, 8, https://doi.org/10.3389/fchem.2020.00315
12. Luo, X., Cheng, H., Wu, X. (2023). Nanomaterials Reinforced Polymer Filament for Fused Deposition Modeling: A State-of-the-Art Review. Polymers, 15, https://doi.org/10.3390/polym15142980
13. Nguyen, K. , Vuillaume, P., Hu, L., López-Beceiro, J., Cousin, P., Elkoun, S., Robert, M. (2023) Recycled, Bio-Based, and Blended Composite Materials for 3D Printing Filament: Pros and Cons—A Review. Mat. Sci. and App., 14, 148-185. https://doi.org/10.4236/msa.2023.143010
14. Pang, X., Yue, S., Huang, S,, Xie, J., Wang, S., Yue, Y., Song, C., Li, D. (2023). Effects of ambient humidity and sintering temperature on the tribological and antistatic properties of PEEK and CF/PEEK. Front. Mater. 10, https://doi.org/10.3389/fmats.2023.1197604
15. Arleo, L., Stano, G., Percoco, G., Cianchetti, M. (2021). I-support soft arm for assistance tasks: a new manufacturing approach based on 3D printing and characterization. Progress in Additive Manufacturing. 6, 1-14. https://doi.org/10.1007/s40964-020-00158-y
16. Mercado-Colmenero, J.M., La Rubia, M.D., Mata-Garcia, E., Rodriguez-Santiago, M., Martin-Doñate, C. (2020). Experimental and Numerical Analysis for the Mechanical Characterization of PETG Polymers Manufactured with FDM Technology under Pure Uniaxial Compression Stress States for Architectural Applications. Polymers, 12. https://doi.org/10.3390/polym12102202

17. Yang, C., Tian, X., Cao, Y., Feng, Z., Changquan, S. (2017). Influence of thermal processing conditions in 3D printing on the crystallinity and mechanical properties of PEEK material. J of Mat. Proc. Tech. 248. https://doi.org/10.1016/j.jmatprotec.2017.04.027
18. Winter, K., Wilfert, J., Häupler, B., Erlmann, J., Altstädt, V. (2022). Large Scale 3D Printing: Influence of Fillers on Warp Deformation and on Mechanical Properties of Printed Polypropylene Components. Macro Molecular Mat. and Eng. https://doi.org/10.1002/mame.202100528
19. Iftekar, S.F., Aabid, A., Amir, A., Baig, M. (2023). Advancements and Limitations in 3D Printing Materials and Technologies: A Critical Review.Polymers 15. https://doi.org/10.3390/polym15112519
20. Korkees, F., Allenby, J., Dorrington, P. (2020). 3D printing of composites: design parameters and flexural performance. Rapid Prototyping Journal. https://doi.org/10.1108/RPJ-07-2019-0188
21. Xiaoyu, B., Runzhou, H. (2022). 3D printing of natural fiber and composites: A state-of-the-art review. Materials & Design, 222, https://doi.org/10.1016/j.matdes.2022.111065
22. Mondal, D., Diederichs, E., Willett, T.L. (2022). Enhanced Mechanical Properties of 3D Printed Nanocomposites Composed of Functionalized Plant-Derived Biopolymers and Calcium-Deficient Hydroxyapatite Nanoparticles. Front. Mater, 9, https://doi.org/10.3389/fmats.2022.833065
23. Bai, W., Fang, H., Wang, Y., Zeng, Q., Hu, G., Bao, G., Wan, Y. (2021). Academic Insights and Perspectives in 3D Printing: A Bibliometric Review. Appl. Sci. 2021, 11, https://doi.org/10.3390/app11188298
24. Li, Z., Yang, C., Burde, E. (2016). An Overview of Biomedical Robotics and Bio-Mechatronics Systems and Applications. IEEE Transactions on Systems, Man, and Cybernetics: Systems. 46. 1-6. https://doi.org/10.1109/TSMC.2016.2571786
25. Kim, G.-T., Go, H.-B., Yu, J.-H., Yang, S.-Y., Kim, K.-M., Choi, S.-H., Kwon, J.-S. (2022). Cytotoxicity, Colour Stability and Dimensional Accuracy of 3D Printing Resin with Three Different Photoinitiators. Polymers 14. https://doi.org/10.3390/polym14050979
26. Golhin, A.P., Tonello, R., Frisvad, J.R., Sotirios, G., Are, S. (2023). Surface roughness of as-printed polymers: a comprehensive review. Int J Adv Manuf Technol 127, 987–1043. https://doi.org/10.1007/s00170-023-11566-z
27. Xu, K., Qin, S. (2023). An Interdisciplinary Approach and Advanced Techniques for Enhanced 3D-Printed Upper Limb Prosthetic Socket Design: A Literature Review. Actuators, 12. https://doi.org/10.3390/act12060223
28. Patpatiya, P., Chaudhary, K., Kapoor, V. (2022a). Reverse Manufacturing and 3D Inspection of Mechanical Fasteners Fabricated Using Photopolymer Jetting Technology. MAPAN 37, 753–763. https://doi.org/10.1007/s12647-022-00561-6
29. Chen, J.V., Dang, A.B.C., Dang, A. (2021). Comparing cost and print time estimates for six commercially-available 3D printers obtained through slicing software for clinically relevant anatomical models. 3D Print Med 7, 1. https://doi.org/10.1186/s41205-020-00091-4
30. Gülcan, O., Günaydın, K., Tamer, A. (2021). The State of the Art of Material Jetting—A Critical Review. Polymers 13. https://doi.org/10.3390/polym13162829
31. Mick, S., Lapeyre, M., Rouanet, P., Halgand, C., Benois-Pineau, J., Paclet, F., Cattaert, D., Oudeyer, P.-Y., de Rugy, A. (2019). Reachy, a 3D-Printed Human-Like Robotic Arm as a Testbed for Human-Robot Control Strategies. Front. Neurorobot. 13, https://doi.org/10.3389/fnbot.2019.00065
32. Krawczuk, M., Palacz, M. (2021). Special Issue “Applications of Finite Element Modeling for Mechanical and Mechatronic Systems”. Applied Sciences, 11. https://doi.org/10.3390/app11115170

33. Andersson, R.,Björsell, N. (2022). The Energy Consumption and Robust Case Torque Control of a Rehabilitation Hip Exoskeleton. Appl. Sci., 12. https://doi.org/10.3390/app122111104
34. Witte, H. (2022). The Interplay of Biomimetics and Biomechatronics. Biomimetics 7. https://doi.org/10.3390/biomimetics7030096
35. Kramberger, A., Gams, A., Nemec, B., Chrysostomou, D., Madsen, O., Ude, A. (2017). Generalization of orientation trajectories and force-torque profiles for robotic assembly. Robotics and Autonomous Systems, 98, 333-346, https://doi.org/10.1016/j.matdes.2022.111065
36. Coyle, S., Majidi, C., Leduc, P., Hsia, K. (2018). Bio-inspired soft robotics: Material selection, actuation, and design. Extreme Mechanics Letters. 22. https://doi.org/10.1016/j.eml.2018.05.003
37. Sanfilippo, F., Økter, M., Dale, J., Tuan, H., M., Zafar, M., H., Ottestad, M. Open-Source Design of Low-Cost Sensorised Elastic Actuators for Collaborative Prosthetics and Orthotics (2023). submitted to HardwareX journal.
38. Sanfilippo, F., Zhang, H., Pettersen K.Y. (2015a). The New Architecture of ModGrasp for Mind-Controlled Low-Cost Sensorised Modular Hands. In Proceeding of the IEEE International Conference on Industrial Technology (ICIT), Seville, Spain, 524–529. https://doi.org/10.1109/ICIT.2015.7125152
39. Sanfilippo, F., Hua, T., Bos, S. (2020). A comparison between a two feedback control loop and a reinforcement learning algorithm for compliant low-cost series elastic actuators. In Proceeding of the 53rd Hawaii International Conference on System Sciences (HICSS 2020), Maui, Hawaii, United States of America, 881–890. https://doi.org/10.24251/HICSS.2020.110
40. Moosavi, S. K. R., Zafar, M. H., Sanfilippo, F. (2022). A Review of the State-of-the-Art of Sensing and Actuation Technology for Robotic Grasping and Haptic Rendering. In Proceeding of the 5th International Conference on Information and Computer Technologies (ICICT), New York City (virtual), United States. https://doi.org/10.1109/ICICT55905.2022.00039
41. https://instructions.online/?id=3988-mechanical%20assembly
42. https://youtu.be/x0tvgowaUfE?si=nHkEfITcb-D-KBVI
43. Gere, J. M., Goodno, B. J. (2012). Mechanics of materials. Boston, Massachusetts: Cengage learning.